

High-speed foil bearings for micro gas turbines: test set-up

P. Vleugels, T. Waumans, J. Peirs., F. Al Bender, D. Reynaerts
Katholieke Universiteit Leuven, Dept. Mechanical Engineering
Celestijnenlaan 300B B-3001 Heverlee, Belgium

Abstract

Mesoscopic or microscopic gas turbines are popular research topics as they could replace batteries. However, a drawback of the miniaturization is the increased rotational speed which should be in the order of 500.000 rpm. Air bearings and more in particular foil bearings are very interesting for application in these units. In this paper we discuss a test set-up to validate our numerical models for foil bearings. This set-up makes it possible to measure the load characteristics of a bearing in a very accurate way since it is based on a 3-bearing configuration. It is known from literature that the clearance value C has a very large influence on the bearing behaviour. Therefore a system to vary the clearance value is proposed. Performing experiments with small clearance variations also allows estimating the initial clearance: an interesting feature as the initial clearance C for flexible geometry bearing, e.g. foil bearings, is hard to measure with sufficient accuracy.

Keywords: PowerMEMS, Microturbine, Foil bearings, Test set-up, Air bearing

1 - INTRODUCTION

Mesoscopic or microscopic gas turbines can be an interesting replacement for batteries as mobile energy supplies. A consequence of small-scale turbomachinery is an increased rotor speed, in the order of 500.000 rpm and higher, making the bearing design a challenging task. Air bearings are the only bearing type able to withstand the severe conditions of high speed and high temperature. However air bearings and more in particular aerodynamic bearings are prone to dynamic instabilities. Therefore unconventional bearing types such as foil bearings may present an interesting solution. A foil bearing, as shown in Figure 1, is comparable with a normal aerodynamic bearing where the rigid journal surface is replaced by a flexible structure. Different solutions e.g. bump type foils [1], advanced plastics [2] and double wound foils [3]; exist in literature as flexible structure. Previous research [4] discussed simulation techniques to predict the steady and dynamic behaviour of foil bearings.

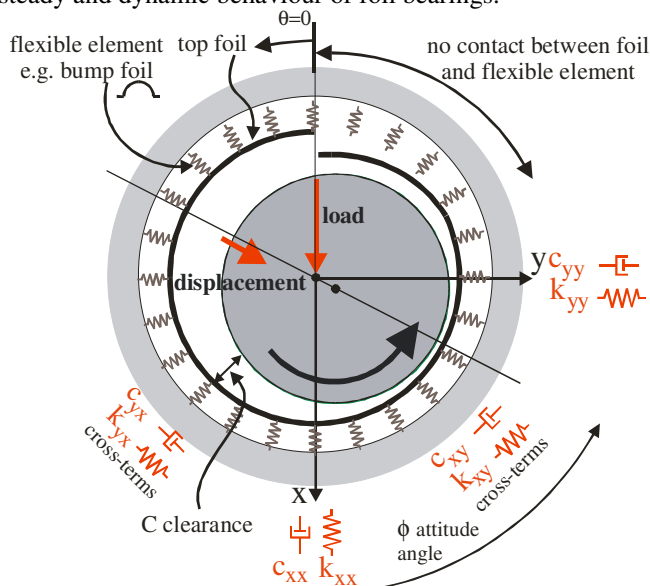


Figure 1 - foil bearing scheme

Figure 2 shows the load capacity W , see eq. (1) in Table 1, of a foil bearing as a function of the bearing number Λ (proportional to speed), see eq. (2) in Table 1, and eccentricity ϵ . for a given L/D -ratio and surface flexibility α . Furthermore, a method to calculate the dynamic properties was proposed. Using the dynamic stiffness and damping coefficients a stability analysis was carried out. This analysis showed that, even without additional (foil) damping, a foil bearing is more stable than a rigid-surface aerodynamic journal bearing with similar geometry but not as stable as generally believed.

This paper describes a test set-up which can be used to validate the previously obtained simulation results. First, the test set-up requirements are defined. In section 3 the concept of the set-up is explained. Section 4 describes in more detail the test set-up. The aerostatic bearing design is discussed in section 5.

2 - TEST SET-UP REQUIREMENTS

The final goal is to achieve a journal bearing which is stable up to (at least) 500.000 rpm in the harsh environment of a micro turbine. The bearing diameter should be in the range of 6 to 8 mm.

Although scale laws permit to test the bearing properties at larger diameters and lower speeds, we opted to perform the experiments with a bearing of diameter 8 mm.

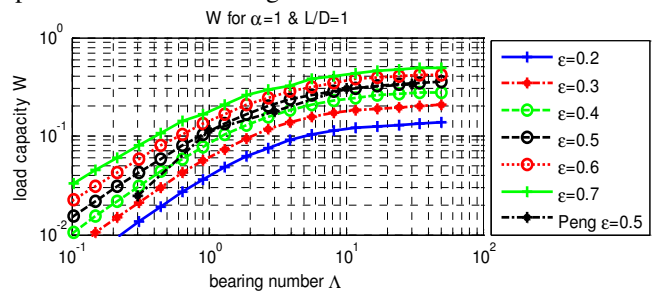


Figure 2 – load capacity W as a function of bearing number Λ and eccentricity ϵ for a given a L/D -ratio and flexibility parameter α

As the maximum speed is the major challenge, designing a test set-up that only provides information about the maximum attainable speed, seems sufficient. However, this speed limit depends on many parameters, making it difficult to draw appropriate conclusions from such experiments. Therefore, an experimental setup able to validate the underlying simulation/calculation models is preferred. Afterwards, a high-speed (prototype) bearing can be selected based on the acquired knowledge.

A first step is the validation of the steady-state load capacity charts, as shown in Figure 2.

Although the validation of the dynamic stiffness and damping properties are not directly envisaged in the current configuration, this can be done by replacing the force application mechanism (see section 4.5 -) by e.g. a shaker.

In order to validate the load charts, a working range as shown in Table 1, for the load W and bearing number Λ is needed. For bearing numbers Λ above 25 compressibility is predominant, resulting in an asymptotic behaviour of the load capacity. Often the maximum achievable speed is a limiting factor (e.g. drive system) in the experiments. For test speeds up to 200.000 rpm and reasonable clearance values of about 10 μm , the bearing number Λ is only 2. This clearly limits the validation range of the load charts. Validation at higher values of the bearing number Λ is only achievable by drastically increasing the rotor speed or decreasing the clearance.

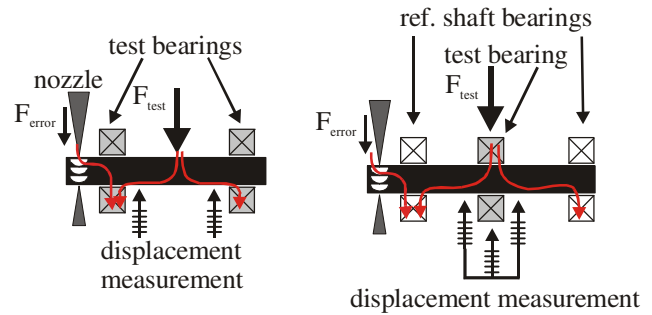
Table 1 – Dimensionless property transformation
with $L=8\text{mm}$ $D=2R=8\text{mm}$ $p_a=1\text{bar}$

	Dimensionless range	Parameter range
Load capacity $W = \frac{F}{p_a LD} \quad (1)$	0.001 .. 1	6.4 mN .. 6.4 N
Bearing number $\Lambda = \frac{6\mu\omega}{p_a} \left(\frac{R}{C}\right)^2 \quad (2)$	0.01 .. 25	If $\omega_{\max}=200.000$ rpm: $C=12 \mu\text{m} \rightarrow \Lambda < 2$ $C=5.6 \mu\text{m} \rightarrow \Lambda < 10$ $C=3.6 \mu\text{m} \rightarrow \Lambda < 25$

3 - TEST APPARATUS CONCEPT

3.1 - 2-bearing vs. 3-bearing configuration

As mentioned earlier the test set-up is intended to validate the foil bearing load charts as shown in Figure 2. Therefore a rotating shaft and a device to apply a force are needed. Often a configuration shown in Figure 3a, from now on called 2-bearing configuration, is used [5]. Hereby an external test force (e.g. from a magnetic actuator or a nozzle) is applied on a shaft supported by two identical test bearings. Either an air turbine or an external motor drive the shaft. An advantage of this configuration is its simplicity because only two bearings are needed and only the test force and shaft displacement have to be measured. However, an additional undesired error



a) 2-bearing configuration b) 3-bearing configuration
Figure 3 – 2-bearing and 3-bearing configuration,

force, e.g. coming from unequal nozzles, can not be identified and is hard to compensate (e.g. nozzle forces are speed dependent).

Therefore a 3-bearing configuration, see Figure 2b is beneficial. In this configuration a reference shaft with two separate bearings is used. Additionally the test bearing is mounted on this reference shaft. After a force is applied on the test bearing, the relative displacement between the shaft and the test bearing has to be measured. Because the displacement of an air bearing is typically not fully inline with the force, this measurement has to be done in the two orthogonal directions.

An error force acting on the shaft does not influence the experimental results, it will only cause an additional shaft displacement. In principle, the stiffness of the reference shaft bearings is not important, nevertheless it is beneficial to design them as stiff as possible. Furthermore production repeatability of the test bearings can be checked as the results of a batch of identical prototypes should give equal results.

3.2 - Clearance C modification

The stability limit of an air bearing scales with the clearance to the fifth power [4]. This indicates that the clearance forms a critical parameter in air bearing design. However, for a flexible geometry bearing, like envisaged in this research, this value is hard to determine sufficiently accurately. Therefore a clearance measurement or clearance identification procedure is needed. Furthermore it is very interesting to test a certain bearing geometry with different clearance values C . This could be done by varying the inner diameter of the prototype bearings or by replacing the shaft with one of different diameter. In case of a 3-bearing configuration it is relatively easy to foresee multiple measurement positions with a stepped diameter shaft.

3.3 - Test set-up concept

Figure 4 shows a schematic of the built test set-up in a 3 bearing configuration. The reference shaft is supported by two aerostatic bearings. The middle section of the shaft has three (slightly) different but well known diameters. It is possible to move to another clearance value by moving the reference shaft and its bearings in vertical direction. As the clearance variation ΔC is known, it is possible to identify the initial clearance C .

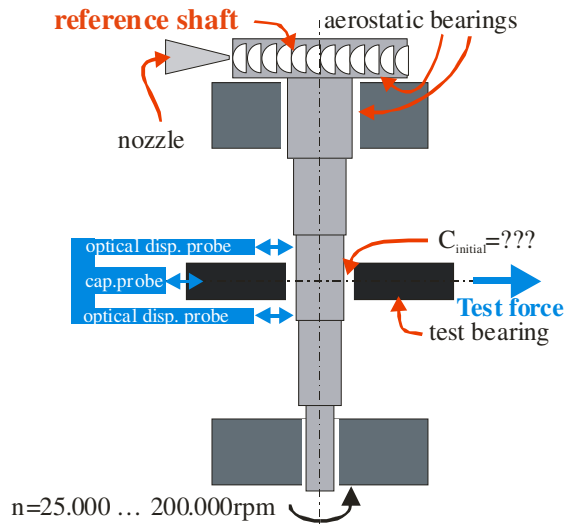


Figure 4 – 3 bearing configuration with a stepped diameter reference shaft.

The relative displacements of the test bearing to the reference shaft is measured by a separate measurement frame fixed to the world. In this frame a capacitive probe measures the displacement of the test bearing, while optical probes measure the displacements of the reference shaft. In order to fulfil Abbe's or Bryan's principle, two optical probes are provided for each direction.

4 - TEST APPARATUS DESCRIPTION

4.1 - General

The reference shaft and its aerostatic bearings are mounted vertically in order to eliminate the gravitational force on the test bearing, see Figure 5a. The expected displacements and forces are small and have to be measured with great accuracy. Therefore, the principles of precision mechanics (kinematic coupling, Abbe-principle ..) are kept in mind during the design.

4.2 - Reference shaft, drive system & aerostatic bearings

The interchangeable reference shaft has three different diameters in its middle section, allowing to test the prototype bearing with three (slightly) different clearance values. The shaft is made from steel 34CrNiMo6 and is electroless nickel plated. Afterwards the shaft is polished in order to obtain a reflective surface needed for the optical probes. Although the shaft is relatively long (80 mm) and slender (average diameter 8 mm) its lowest eigenfrequency is at 280.000 rpm, well above the maximum targeted maximum speed of 200.000 rpm

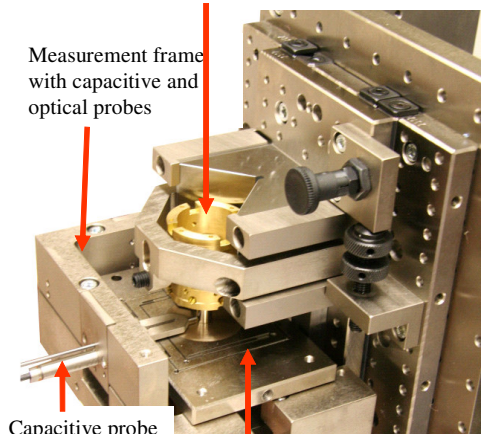
The reference shaft bearings for both journal and thrust direction are aerostatic bearings. More information about the calculation can be found in section 5 -.The shaft is driven by two stationary nozzles and a small impulse turbine machined on the shaft.

The complete reference shaft unit, consisting of the aerostatic bearing blocks, the reference shaft, the drive system and the V-block on which the aerostatic bearing blocks are mounted, is assembled on a crossed V-slider. This allows vertical shifting of the complete unit with respect to the test bearing. The test bearing and the measurement system for both displacement and force are fixed to the world.

4.3 - Test bearing support

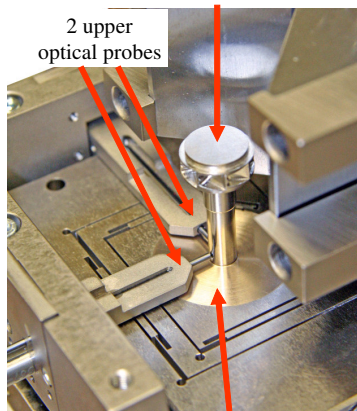
The test bearing is mounted in a flexible leaf spring structure shown in Figure 5b. This structure allows movement in two degrees of freedom. The leaf springs are designed to have a stiffness of 2 N/mm in both directions. Although the positioning between the reference shaft unit and the test bearing support is done with location pins (DIN 6321) and 3 balls, it is unlikely that the alignment of the test bearing with the reference shaft is perfectly concentric. Even the smallest positioning error has a significant influence as the clearance value is in the range of $10\mu\text{m}$. Through the flexible leaf springs this positioning error will act as a small bearing preload.

Upper aerostatic bearing block with reference shaft mounted in a V-block on a crossed slider



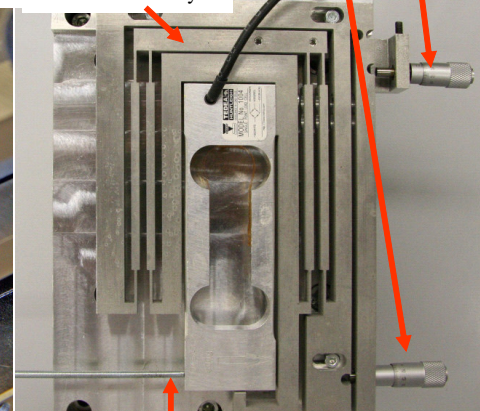
Test bearing mounted in the test bearing support
a) General view on test set-up (force sensing and application not shown)

Reference shaft with the turbine and thrust bearing (upper aerostatic bearing block removed)



Test bearing in test bearing support (dummy prototype installed)
b) measurement frame and the test bearing support (leaf springs allowing movement in 2 degrees of freedom)

Micrometer screws to move intermediate body
Intermediate body



Force sensor with coupling rod to test bearing
c) force application and sensing mechanism, made of a double compound leaf spring mechanism and force sensor integrated.

Figure 5 Test set-up

4.4 - Displacement measurement system

A disadvantage of the chosen 3-bearing configuration is the need for differential measurements. Both the reference shaft movement and the test bearing movement have to be measured. Typically the displacement of an air bearing is not fully inline with the applied force. Therefore, the displacement measurements have to be done in two orthogonal directions. The movements of the test bearing are measured with Lion capacitive probes. The reference shaft displacements are measured with an in-house developed optical measurement system.

4.5 - Force application & measurement

A mechanism, see Figure 5c, basically a double compound leaf spring mechanism, is designed to load the test bearing. Two micrometer screws (one for rough and one for fine positioning) move the intermediate body, which is connected to the world by the two outer leaf springs. When the intermediate body moves while the connecting rod to the test bearing is standing still, a test force is generated by the inner two leaf springs. Furthermore, a force sensor type 1004 600 gr from Tedeo Huntleigh, based on strain gauges and notch type flexible joints, is integrated. The maximum force which can be applied is 6 N. The leaf springs are sufficiently flexible such that the small displacements of the test bearing due to a change in load carrying capacity with speed are negligible.

5 - AEROSTATIC BEARING DESIGN

As already mentioned, aerostatic journal and thrust bearings are used to support the reference shaft. Each bearing contains eight inherent restriction feedholes. The bearing behaviour is modelled by a finite difference discretisation of the compressible Reynolds equation. At feedhole nodes suitable boundary conditions are applied by using a lumped-parameter formulation of the entrance flow effects.

This formulation relies on the analytical solution of the boundary layer equations describing the entrance flow by separating the velocity into an amplitude and a profile function [6-7]. Obtained solution data makes it possible to tabulate a coefficient of discharge C_d which corrects the ideal entrance flow.

The dynamic stiffness and damping coefficients are calculated by a perturbation method [8]. As the current test set-up is intended for measuring the steady state behaviour, the static stiffness is the most important.

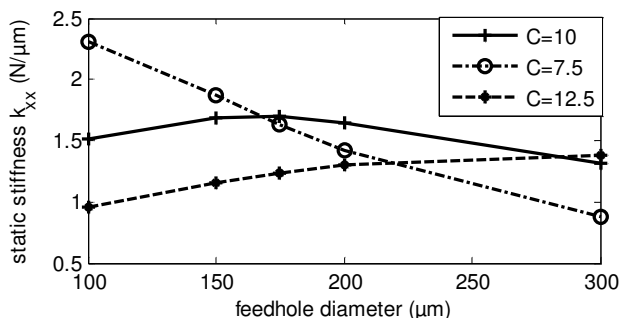


Figure 6 Static stiffness of aerostatic bearings for $D=8$ mm L/D -ratio=1, 8 feedholes, $p_{supply}=6$ bara

Figure 6 shows the static direct stiffness terms k_{xx} for several clearance C and feedhole combinations. The highest stiffness can be achieved by using a small clearance (e.g. 7.5 μm) in combination with a small feedhole diameter (e.g. <100 μm). However, these small dimensions result in very stringent manufacturing tolerances. Therefore a clearance value of 10 μm in combination with a feedhole of 175 μm is chosen.

6 - CONCLUSION

A test set-up to validate previous simulations on foil bearings is designed and almost operational. Special attention is drawn to measurement accuracy by using the precision engineering principles and a 3-bearing configuration. Aerostatic bearings are used for the reference shaft. The method to vary the clearance is integrated, making it possible to identify the initial clearance. The coming period will be used for commissioning and carrying out a system test program. Afterwards the experiments can start.

ACKNOWLEDGMENTS

This research is sponsored by the Institute for the Promotion of Innovation by Science and Technology in Flanders, Belgium, project SBO 030288, and by the Belgian programme on Interuniversity Poles of Attraction (IAP5/06: AMS). Also, this work was carried out within the framework of the EC Network of Excellence "Multi-Material Micro Manufacture: Technologies and Applications (4M)". Dr Jan Peirs wishes to acknowledge the Industrial Research Fund K.U.Leuven. T. Waumans has a research scholarship of the Fund for Scientific research Flanders.

REFERENCES

- [1] Heshmat H., Walowit J.A., Pinkus O., "Analysis of Gas-Lubricated Foil Journal Bearings", *J Lubric Tech-T ASME*, Vol 105, pp. 647-655, 1983
- [2] Hou Y., Zhu Z.H., Chen C.Z., "Comparative test on two kinds of new compliant foil bearing for small cryogenic turbo-expander", *Cryogenics*, Vol 44, pp. 69-72, 2004
- [3] Kitazawa S., Kaneko S., Watanabe T., "Prototyping of Radial and Thrust Air Bearing for Micro Gas Turbine", *Proc. of IGTC2003*, Tokyo, TS-019
- [4] Vleugels P., Waumans T, Peirs J, Al-Bender F., Reynaerts D., "High-speed bearings for micro gas turbines: stability analysis of foil bearings", *J. Micromech. Microeng.* Vol. 16, No 9, pp. 282-289, September 2006.
- [5] San Andres L., Rubio D., Ho Kim T., "Rotordynamic performance of a rotor supported on bump type foil gas bearings: experiments and predictions", *ASME GT2006-91238*, Barcelona, Spain, May 8-11, 2006
- [6] Al-Bender F., Van Brussel H., "A method of 'separation of variables' for the solution of laminar boundary-layer equations of narrow-channel flows", *J Tribol-T ASME*, Vol. 114, pp 623-629, July 1992
- [7] Al-Bender F., Van Brussel H., "Symmetric radial laminar channel flow with particular reference to aerostatic bearings", *J Tribol-T ASME*, Vol. 114, pp 630-636, July 1992
- [8] Waumans T, Vleugels P., Peirs J, Al-Bender F., Reynaerts D., "Rotordynamic behaviour of a micro-turbine rotor on air bearings: modeling techniques and experimental verification Rotordynamic", ISMA Conf., ID 571, Leuven, Sep. 18-20, 2006 *J. Micromech. Microeng.* Vol. 16, No 9, pp. 282-289, September 2006.